Astron. Astrophys. 324, 1071–1082 (1997)

ASTRONOMY
AND
ASTROPHYSICS

Analytical 2-D solutions for hydrodynamic, thermally and radiatively driven, astrophysical outflows. Applications to B stars

Alexander Kakouris[1,2] **and Xenophon Moussas**[1]

[1] Space Group, Section of Astrophysics, Astronomy and Mechanics, Physics Department, National University of Athens, Panepistimiopolis GR-15783, Athens, Greece (akakour@atlas.uoa.gr, xmoussas@atlas.uoa.gr)
[2] Hellenic Air Force Academy, Dekelia, Attiki, Greece

Received 25 March 1996 / Accepted 31 January 1997

Abstract. In this work, we deal with the two-dimensional problem of steady plasma outflow from rotating central astrophysical gravitational objects. Considering the stellar atmosphere optically thin and the radiative force (due to the central object's luminosity) radial, we obtain fully analytical solutions for thermally and radiatively driven outflows. The flow is helicoidal and axisymmetric and the plasma inviscid and non-polytropic. First, we generalize the Kakouris & Moussas 1996 solution imposing a generalized geometry in the flow velocity which implies differential fluid rotation. The solutions are of four types with velocity maxima either along the equator or along the polar axis of the central body. The dependence of the solutions upon the radial distance R is similar to Kakouris & Moussas 1996 case for each type of solutions. Just assuming that the radiative acceleration is a function of the distance we obtain analytical 2-D solutions for thermally and radiatively driven outflows. The inclusion of the radiative force helps the generation of the stellar wind giving higher maximum radial velocities. The velocity asymmetry between the equator and the poles varies with radial distance and it is sensitive upon the relative strength of the adopted radiative force as well as upon the degree of the fluid differential rotation. Several possible dependences of the radiative acceleration upon the radial distance are considered, and the deduction of the wind transition from a strong radiative driving to a pure non-radiative thermally driven outflow is presented by the given applications.

The incorporation of the radiative force in the hydrodynamic equations is very important in massive winds of early and late type main sequence stars and evolved giants and supergiants. We present analytical 2-D solutions for thermally plus radiatively driven stellar winds and we apply one kind of them to B5I type supergiants in order to understand the observed winds of these stars under a thermal (coronal) plus a radiative mechanism of ejecting stellar plasma in the interstellar medium. Maximum outflow velocities and mass loss rates, close to the observed, are easily obtained.

Send offprint requests to: A. Kakouris

Key words: hydrodynamics – stars: winds – atmospheres – flows – radiation pressure – methods: analytical – B supergiants: winds – atmospheres – mass-loss

1. Introduction

The subject of the steady mass outflow from gravitating stellar objects or the problem of steady mass infall or accretion around them is widely studied after Parker's original work for the solar wind (1958) and Bondi's work for spherical accretion (1952). The previous models are one-dimensional (1-D) but the phenomena are observed to need at least two-dimensional (2-D) interpretation (i.e the flow quantities vary between the equator and the poles of the central object). The last remark was recently validated for the solar wind by Ulysses *in situ* measurements (Phillips et al. 1995) and is also observed in all astrophysical scales and for the majority of stars, planetary nebulae, active galactic nuclei (AGNs) and quasars (Cassinelli 1979, Hughes 1991, Sauty 1994, Bryce et al. 1994). In order to model the observed global hydrodynamic (HD) flows, either numerical solutions or analytical results and exact solutions are used.

Analytical 2-D, self-consistent solutions to the hydrodynamic outflow from central astrophysical objects have been presented by Tsinganos & Vlastou 1988, Tsinganos & Trussoni 1990, Tsinganos & Sauty 1992, Lima & Priest 1993 and Kakouris & Moussas 1996. The flow is axisymmetric and helicoidal in all previous cases except Tsinganos & Sauty model in which the streamlines initially flare to the equator or initially concentrate to the poles giving always radial asymptotes at large distances. Lima & Priest generalized the Tsinganos & Trussoni model obtaining initially large velocity differences between the equator and the poles and radial asymptotes. Their solution is a set of general separated variables functions and recently, Lima & Tsinganos 1996 fit the Ulysses off-the-ecliptic plasma measurements with their 2-D analytical results. The Kakouris & Moussas 1996 solution (hereafter KM or Paper I) are non-separated variables, fully analytical, and describe 2-D helicoidal

and axisymmetric, thermally driven flows. A disadvantage of this model is the large initial radial velocity which is needed for the outflow from some types of stars. Including the radiative force in this paper, we diminish the initial flow velocity to realistic very low values.

In this work we generalize the Paper I solution taking into account the differential rotation of the fluid. The steepening of the rotating area around the equatorial plane is controlled by a free parameter and the behaviour of the solutions upon it is deduced in Sect. 2.1. Moreover, we study the effect of a radiative force in the governing HD equations and using the previous solution we derive analytical solutions for a 2-D thermally and radiatively driven stellar wind (Sect. 2.2). As a result, lower initial velocities and larger acceleration are obtained. The first radiatively driven wind model was presented in 1975 by Castor, Abbott & Klein. The authors presented numerical solutions for early type star's outflows. In the same article a first definition of the radiative force is given. This original numerical work, usually referred as CAK model, led to several subsequent works which improved the theory of radiatively driven winds presenting applications to stellar winds from evolved stars as well. Nowadays there is a wide literature of the radiation-driven winds and some of these works (used or discussed in this paper) have been presented by Abbott 1982, Lamers 1986, Poe & Friend 1986, Araujo & Freitas Pacheco 1989, Kudritzki et al. 1989, Kudritzki 1992, Chen et al. 1992, Koninx & Hearn 1992, Bjorkman & Cassinelli 1993, Chen & Marlborough 1994, Owocki et al. 1994, Gonzalez et al. 1995, Araujo 1995, de Kool & Begelman 1996. In this work we derive analytical solutions considering a generalized *radiation law* and we apply them (Sect. 3) in evolved B5I type supergiants calculating a mass loss rate of $\dot{M} = 3.7\ 10^{-7}\ M_{\odot}/yr$. The maximum outflow velocities, for the given application, range from 200 to 800 km/sec. In Sect. 4 we summarize the results and discuss the model physical characteristics in explaining the observed mass-loss from massive stars compared with the 1-D or 2-D radiatively driven models already mentioned.

2. Basic equations and solutions. The effect of the radiation pressure

Equations (1, 2, 3) represent the 3-D steady ($\partial/\partial t = 0$), non magnetized outflow of an inviscid, ideal, compressible fluid from a gravitational central object, conserving mass, momentum and energy:

$$\nabla(\rho\mathbf{u}) = 0 \tag{1}$$

$$\rho[\mathbf{u}\cdot\nabla]\mathbf{u} = -\nabla P + \mathbf{F}_{rad} - \rho\frac{\mathrm{G}M}{r^2}\widehat{r} \tag{2}$$

$$[\mathbf{u}\cdot\nabla](\frac{P}{(\gamma-1)\rho}) + P[\mathbf{u}\cdot\nabla](\frac{1}{\rho}) = \sigma \tag{3}$$

This set of partial nonlinear differential equations is completed by an equation of state for a fully ionized hydrogen plasma:

$$P = 2\frac{k_B T\rho}{m_p} \tag{4}$$

The symbols have the usual meaning, i.e. r is the radial distance, $\mathbf{u}$ is the flow velocity, ρ is the flow density, P is the flow pressure, T is the flow temperature, G is the gravitational constant, M is the mass of the central gravitational body, k_B is the Boltzmann's constant, m_p is the mass of the proton, γ is the ratio of the specific heats and σ is the rate of any external energy addition per unit of fluid mass. The $\mathbf{F}_{rad}$ in Eq. (2) is the specific radiative force due to the luminosity of the central object.

2.1. Non-radiative solutions with differential rotation

Without the radiative force $\mathbf{F}_{rad}$ and supposing axisymmetry ($\partial/\partial\phi = 0$) in spherical coordinates (r, θ, ϕ) (θ the polar angle measured from the rotational axis) and helicoidal geometry for the streamlines ($V_\theta = 0$), we can derive (similar to Kakouris & Moussas 1996) analytical solutions of the form:

$$V_R(R,\theta) = \sqrt{f(R) - (g(R) + \frac{\omega^2}{R^2})\sin^{2\mu}\theta},$$

$$V_\phi(R,\theta) = \frac{\omega\sin^{\mu}\theta}{R} \tag{5}$$

where μ is a constant and the velocities are measured in thermal velocity parameter units V_p

$$V_p = \sqrt{\frac{2k_B T_p}{m_p}} \tag{6}$$

with T_p a temperature parameter, the radial distance R in stellar radii R_o and ω is the dimensionless azimuthal velocity at the equatorial surface of the star. The full derivation of the new solutions is given in Appendix A.

ω is a parameter in the model increasing with the rotation of the central object $\omega = V_{rot}(\theta = \pi/2)/V_p$. Another dimensionless parameter appearing in the solutions is ν which represents the ratio of the escape velocity V_{esc} at the stellar surface to the thermal velocity parameter V_p:

$$\nu = \frac{V_{esc}}{V_p} = \sqrt{\frac{2\mathrm{G}M/R_\mathrm{o}}{2k_B T_p/m_p}} \tag{7}$$

As seen from Eqs. (5) the new solutions introduce *differential rotation* for the fluid and generalize the Paper I case including a new parameter μ (hereafter called as *differential rotation parameter*) which controls the steepening of the rotating region. In this way, the Paper I solution becomes a special case of these generalized solutions for $\mu = 1$ illustrating solid body rotation for the fluid. The dependence of V_ϕ upon μ is shown in Fig. 1 where the solid body rotation is shown by the thick line.

In the helicoidal case ($V_\theta = 0$) the mass conservation (Eq. 1) is satisfied by the following density function:

$$\rho(R,\theta) = \frac{\rho_o}{R^2 V_R(R,\theta)} \tag{8}$$

with ρ_o a dimensional constant while the azimuthal velocity function given by (Eq. 5) conserves the angular momentum,

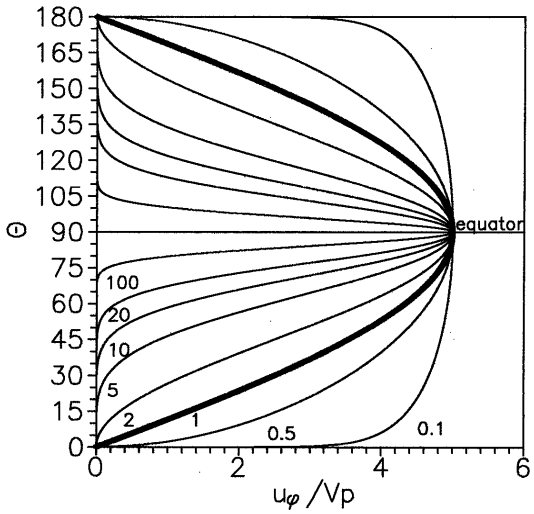

Fig. 1. Differential fluid rotation described by Eq. (5). The dependence of the dimensionless azimuthal velocity upon the colatitude θ at the stellar surface for several values of the exponent μ (μ = 0.1, 0.5, 1, 2, 5, 10, 20 ,100). Increasing μ steepens the fluid rotating area close to the equatorial plane.

satisfying the ϕ-component of the force balance equation (2). Moreover, the free functions $f(R)$ and $g(R)$ of Eq. (5) are found (Appendix A) to be:

$$f(R) = f_{\rm o}(R)[A + A_1 I_1] \tag{9}$$

$$g(R) = \frac{\xi - (\mu+1)\omega^2}{\mu\, R^2} \tag{10}$$

where A is a constant, $A_1 = c\nu^2/2$,

$$f_{\rm o} = \frac{|\xi - \omega^2|^{\frac{2(\mu+2)}{\mu+3}}}{|\xi - 2\omega^2|^{\frac{2\mu}{\mu+2}} |\xi - (\mu+4)\omega^2|^{\frac{2(\mu+4)}{(\mu+3)(\mu+2)}}} \tag{11}$$

and I_1 is an integral (evaluated by Simpson's rule):

$$I_1 = \int Y_1 d\xi \tag{12}$$

with

$$Y_1(\xi) = \frac{-\xi}{(\xi - (\mu+4)\omega^2)(\xi - 2\omega^2)} \cdot \frac{|\xi - (\mu+4)\omega^2|^{-\frac{(\mu-2)(\mu+4)}{2(\mu+3)(\mu+2)}} |\xi - 2\omega^2|^{\frac{2\mu}{\mu+2}}}{|\xi - \omega^2|^{\frac{4\mu+7}{2(\mu+3)}}} \tag{13}$$

The new variable ξ is related to the radial distance R as:

$$(cR)^{2\mu+6} = \frac{|\xi - (\mu+4)\omega^2|^{\mu+4}}{|\xi - \omega^2|} \tag{14}$$

with c a constant which normalizes the solution at the stellar surface. So, the radial V_R and the total V flow velocity are written as

$$V_R = \sqrt{f(R) - \frac{\xi - \omega^2}{\mu R^2} \sin^{2\mu}\theta} \tag{15}$$

$$V = \sqrt{V_R^2 + V_\phi^2} =$$

$$\sqrt{f_{\rm o}[A + A_1 I_1(\xi)] - \frac{\xi - (\mu+1)\omega^2}{\mu\, R^2} \sin^{2\mu}\theta} \tag{16}$$

The new solutions are of four types named as solution in *Region I-IV* respectively (similar to Paper I, see Appendix A). The radial velocity maximum occurs along the equator of the central object in Ranges I,II and along the polar axis in Ranges III,IV. The solutions in Ranges II-IV are inappropriate for stellar wind interpretation (see discussion of Paper I) and they could be examined only as inflows. The dependence of the solutions upon the parameters (except μ) is the same with Paper I. So, we discuss the behaviour of the solutions upon the new parameter μ.

In Range I ($-\infty < \xi \leq 0$) the solution represents an outflow which starts subsonic at the stellar surface and terminates supersonic at infinity. The initial radial velocities at the central object's surface (equatorial $u_{in/e}$ and polar $u_{in/p}$) are obtained by Eq. (5) for $\xi = 0$:

$$u_{in/e} = u_R(R=1, \theta = 90^o) = V_p \sqrt{f_{\rm o}(\xi=0)A + \frac{\omega^2}{\mu}}$$

$$u_{in/p} = u_R(R=1, \theta = 0^o) = V_p \sqrt{f_{\rm o}(\xi=0)A} \tag{17}$$

where

$$f_{\rm o}(\xi=0) = \frac{1}{2^{\frac{2\mu}{\mu+2}} (\mu+4)^{\frac{2(\mu+4)}{(\mu+2)(\mu+3)}}} \tag{18}$$

The variation of $f_{\rm o}(\xi = 0)$ with μ is negligible ($f_{\rm o}(\xi = 0) \rightarrow 4^{-4/3}$ when $\mu \rightarrow 0$ and $f_{\rm o}(\xi = 0) \rightarrow 4^{-1}$ when $\mu \rightarrow \infty$). We see that the initial velocities increase with the parameter A while the initial velocity asymmetry at the stellar surface depends on the ratio ω^2/μ. This means that by increasing the rotation (ω) or decreasing the differential rotation parameter (μ) we obtain larger initial velocity asymmetry at the stellar surface.

The behaviour of the radial velocity upon the new parameter μ is shown in Fig. 2. As seen, the increase of μ produces higher velocities and decreases the flow asymmetry. The μ change leads to redistribution of the azimuthal velocity values without changing the polar and equatorial ones according to Eq. (5) (Fig. 1). So, the μ increase produces lower azimuthal velocity for a given θ. The respective radial velocity increases.

In order to understand the previous behaviour we write the dimensionless outward radial acceleration (in units $V_p^2/R_{\rm o}$):

$$a_R^{out} = a_{\rm therm} + a_{\rm centr} + a_{\rm grav} = -\frac{\rho_o}{\rho}\frac{\partial P}{\partial R} + \frac{V_\phi^2}{R} - \frac{\nu^2}{2R^2} \tag{19}$$

Substituting the several expressions (Appendix A) we get:

$$a_R^{out} = \frac{1}{2}\frac{{\rm d}f}{{\rm d}R} - \left(\frac{1}{2}\frac{{\rm d}g}{{\rm d}R} - \frac{\omega^2}{R^3}\right)\sin^{2\mu}\theta \tag{20}$$

and replacing $f(R)$ and $g(R)$ from Eqs. (9, 10) we finally obtain:

$$a_R^{out} = a_{SS}(\xi) + a_{Non-SS}(\xi)\sin^{2\mu}\theta =$$

$$-\frac{\nu^2}{2R^2}\frac{\xi-\omega^2}{\xi-2\omega^2} + \frac{2\omega^2}{R}\frac{-2\xi+(\mu+4)\omega^2}{\xi(\xi-2\omega^2)} f +$$

$$\left(\frac{\mu+4}{\mu}\right)\left(\frac{\xi-\omega^2}{\xi}\right)\frac{\omega^2}{R^3}\sin^{2\mu}\theta \qquad (21)$$

where $a_{SS}(\xi)$ denotes the spherically symmetric terms and a_{Non-SS} the non - spherically symmetric. Note that in Range I the first symmetric term is negative (decelerating term) and it is proportional to gravity and independent of the fluid differential rotation (μ). All the other terms are positive (accelerating) and diverge near the stellar surface ($\xi \to 0$). This means that the thermal pressure force is capable to excite any stellar wind but increases enormously at the stellar surface for some values of the parameters (large μ contributes this behaviour, second symmetric term). The coefficients of the non symmetric term show that the asymmetry increases with the rotation (ω) and decays with the degree of the differential rotation (μ) ($\mu+4/\mu$ diverges when $\mu \to 0$ and tends to unity when $\mu \to \infty$). The evolution of the symmetric term $a_{SS}(\xi)$ with μ is shown in Fig. 2 by the polar curves (b) ($\theta = 0$). High degree of differential rotation produces higher velocities by increasing the flow acceleration near the stellar surface. This result is also found by Lima & Priest 1993 and it is consistent with the Bernoulli's law because, an increase in μ diminishes the azimuthal velocity at a given θ and increases the radial, so, the total velocity (Eq. 16) tends to remain constant (it is not constant because of external heating/cooling). Moving towards the equator at the same distance the non - symmetric acceleration term is added (the centrifugal and the non symmetric part of the thermal pressure force are added in the force balance) so, higher radial velocities are obtained and the non - symmetric contribution becomes more important for lower values of μ (Fig. 2, for $\mu = 0.1$ we obtain the largest equatorial radial velocities and the highest asymmetry, curves 1).

Setting $\mathscr{A} = 0$ in the pressure expression (Appendix A, Eq. A2) the pressure vanishes at infinity. In this case, the radial Mach number (defining the speed of sound as $V_s = \sqrt{\gamma P/\rho}$, Appendix A, Eq. A4) is spherically symmetric starting from a value of 0.77 at the stellar surface and increasing with the radial distance. So, the flow originates subsonic, passes a spherical sonic surface and terminates supersonic at infinity. The radius of the spherical sonic surface is:

$$R_s = \frac{1}{\sqrt{3}\,5^{\frac{1}{2\mu+6}}}\left(\frac{3\mu+14}{\mu+4}\right)^{\frac{\mu+4}{2\mu+6}}$$

and the deduction of the last equation shows that R_s decays with μ. It is $R_s = 1.018$ (in stellar radii) when $\mu = 0$ and $R_s \to 1$ when $\mu \to \infty$ ($R_s = 1.014$ when $\mu = 1$, Paper I). So, the increase of the differential rotation degree (μ) shortens the subsonic region above the star's surface and in a highly differentially rotating outflow the sonic surface tends to coincide with the stellar surface. In this case the wind tends to originate (super)sonic.

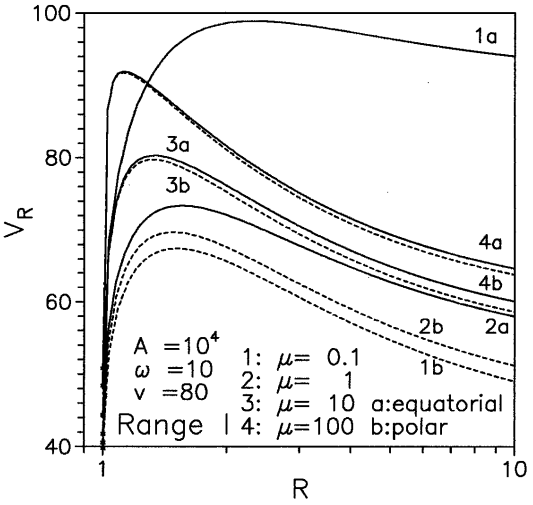

Fig. 2. Dependence of the Range I dimensionless radial velocity V_R upon the differential parameter μ for fixed values of the rest parameters $A = 10^4, \omega = 10, \nu = 80$. Equatorial profiles are shown with solid curves an the polar with the dashed. It is seen that the increase of the parameter μ reduces the θ - asymmetry of the flow.

In conclusion, the new solutions differ from Paper I in the generalized differential fluid rotation. The concentration of the rotation at the equator ($\mu >> 1$) produces a smaller subsonic region close to the stellar surface with stronger radial acceleration. Moreover, the area of fluid heating around the star follows the decay of the subsonic region.

2.2. Inclusion of the radiative force

In order to apply the model in the atmospheres of massive stars where the radiation pressure is significant, due to absorption of the light in the expanding corona, a radiation force $\mathbf{F}_{rad}$ per unit of the fluid volume can be included in the model (Eq.2). The radiative mechanism is supposed to be dominant in many cases so radiatively driven wind models have been developed. Of course, a strict interpretation of radiatively driven winds demands calculation of the exact radiative force. This force must be defined by the full theoretical study of the light propagation in plasmas as well as by spectroscopic observations of the stellar atmospheres.

On the other hand, the radiative force is expected to depend on the radiation wavelength λ differing in each absorption line and in the continuum of the stellar spectrum. So, the chemical composition, the temperature and the ionization stage of the stellar atmosphere is crucial in the absorption mechanisms. It raises from the previous work that the total radiative force can be separated in three parts: the continuum, the thick and the thin lines contributions:

$$F_{rad} = f_{rad}^{C} + f_{rad}^{ThickLines} + f_{rad}^{ThinLines} \qquad (22)$$

The continuum contribution due to Thomson scattering of the photons by the free plasma electrons, giving an acceleration inversely proportional to the squared distance and proportional

to the star's luminosity L. This part of the force usually is added to gravity leading to an *effective gravity* reduced by a factor $(1-\Gamma)$ with

$$\Gamma = \frac{L\sigma_T}{4\pi c \mathrm{G} M}$$

where σ_T is the Thomson electron scattering cross section and c the speed of light.

CAK use an expression for the line radiative force of the form:

$$f_{rad}^{lines} = \rho \frac{\sigma_e L}{4\pi c R^2} M(t) \tag{23}$$

where σ_e is Thomson scattering coefficient of the free electrons per unit mass, t is an optical depth variable ($t = \rho\sigma_e u_{th}/(\partial V_R/\partial R)$, with u_{th} the electron thermal velocity) and $M(t)$ is a force multiplier representing the effect of all lines. The multiplier was defined as

$$M(t) = kt^{-\alpha}$$

where k measures the number of contributing lines and α characterizes the relative importance of optically thin to optically thick lines (for $\alpha = 0$ only optically thin lines contribute and for $\alpha = 1$ only optically thick). The line radiative force was extensively discussed by Abbott 1982 and after corrections made (dilution factor w, exponent δ) due to the radial variance of the photoionization-recombination balance and after the finite cone angle correction $CF(R, V_R, \partial V_R/\partial R)$ (Friend & Abbott 1986, Kudritzki et al. 1989) the line radiative force yields:

$$f_{rad}^{lines} = \rho \frac{\sigma_e L}{4\pi c R^2} M(t) \left(\frac{n_e}{W}\right)^{\delta} CF \tag{24}$$

where n_e is the electron number density.

In the definition of the line radiative force and especially for the case of optically thick lines, the Sobolev approximation has been adopted which states that the lines are desaturated by large Doppler shifts. So the force depends on the radial velocity and its gradient. However, Lamers 1986 discussed the validity of such approximation for the massive but low radial velocity wind of P Cygni pointing out that the Sobolev approximation is valid only when $dV_R/dR >> u_d/R_\mathrm{o}$ where u_d is the Doppler velocity due to thermal and turbulent motion. After estimations he concluded that Sobolev approximation is not valid for such winds and he derived a different formula. The radiative force in the case of optically thin atmosphere has also been discussed by Chen & Marlborough 1994 showing that it can be written as a power law of radial distance. We shall use this result in the following section. Recent work in determining the radiative acceleration concerning several absorption mechanisms presented by Gonzalez et al. 1995. de Kool and Begelman 1996 derived recently self-similar 2-D solutions to radiation pressure driven magnetic disk winds, using the optically thin atmosphere hypothesis and an inverse squared distance radiative law. In optically thick atmospheres and using the Sobolev approximation, powerful numerical solutions and simulations have been developed.

In this work, we consider a radial outward *mean radiative force* over the wavelengths (continuous absorption and individual absorption lines) $F_{rad} = \int_0^\infty F_\lambda d\lambda$. We also suppose that the force is independent from the flow velocity and its gradient (i.e. no Sobolev approximation for optically thick absorption lines). This assumption is appropriate to an *optically thin* stellar atmosphere ($\alpha = 0$, Eq. 23) or to conditions where the Sobolev approximation collapses (Lamers 1986). Moreover, the radiative force should be proportional to the fluid density ρ since the absorption increases with it, and the radiative acceleration ($a_{rad} = F_{rad}/\rho$) is supposed to be spherically symmetric:

$$\mathbf{F}_{rad} = F_o \, \frac{\rho(R,\theta)}{\rho_o} \, Q(R) \, \widehat{r} \tag{25}$$

where F_o is a constant and $Q(R)$ an *arbitrary* positive function of the radial distance. The function $Q(R)$ is expected to decay with radial distance R as the stellar corona expands. The factor F_o is proportional to the luminosity of the central object L and also depends on the photon scattering mechanism. Both F_o and $Q(R)$ are also affected by the abundance of the various species (ions) in the plasma and the ionization degree which determine the scattering mechanism. For example, if the fluid consists of fully ionized hydrogen plasma and the light absorption is taking place through pure Thomson scattering with the electrons then:

$$F_o = \frac{L\sigma_T\rho_o}{4\pi c R_\mathrm{o}^2 m_p} = \frac{L}{L_E}\frac{\mathrm{G}M}{R_\mathrm{o}^2}\rho_o, \quad Q(R) = \frac{1}{R^2}$$

where L_E the Eddington lumimosity:

$$L_E = \frac{4\pi \mathrm{G} M m_p c}{\sigma_T} \tag{26}$$

Using the radiative force described by (25) the $f(R)$ function of the solutions becomes:

$$f(R) = f_\mathrm{o}(R)[A + A_1 I_1 + A_2 I_2] \tag{27}$$

where $A_2 = F_o m_p R_\mathrm{o}/(2k_B T_p \rho_o)$ and $I_2(\xi) = \int Y_2 \mathrm{d}\xi$ with:

$$Y_2(\xi) = \frac{RQ(R)\xi}{(\xi-(\mu+4)\omega^2)(\xi-2\omega^2)} \cdot$$
$$\frac{|\xi-(\mu+4)\omega^2|^{\frac{2(\mu+4)}{(\mu+3)(\mu+2)}}|\xi-2\omega^2|^{\frac{2\mu}{\mu+2}}}{|\xi-\omega^2|^{\frac{2(\mu+2)}{(\mu+3)}}} \tag{28}$$

The integral I_2 has always opposite sign with I_1.

It is seen from Eq. (27) that the *fully analytical 2-D solution* for a thermally and radiatively driven stellar wind requires a *radiative law* $(F_o, Q(R))$.

In Fig. 3 an application of *Range I* radiative solution with the radiative force incorporated is shown in comparison with the non-radiative (KM solution with $\mu = 1$). The central object is a supergiant star (e.g. K5I) with:

$$M = 12\ M_\odot,\ R = 400\ R_\odot,\ V_{rot} = 25\ km/sec$$

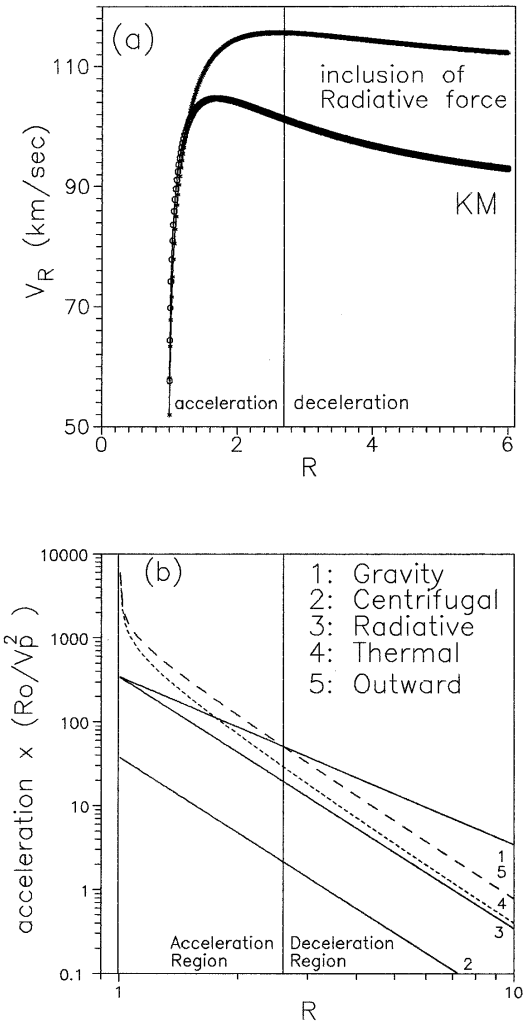

Fig. 3a and b. Radiative and nonradiative (KM or Paper I) *Range I* solutions with the same set of parameters for a K5I supergiant. (**a** radial velocity profiles **(b** dimensionless accelerations for the radiation-included solution (gravity (1) is the unique inward force while the outward force (5) is the total sum of the thermal (4), centrifugal (2) and radiative (3) forces) The *acceleration* and *deceleration* regions refer to the radiation included solution. It is seen that even a "minimal" radiation law produces significant acceleration close to the star.

and we use model parameters: $T_p = 10^3\ K$ (which gives $\sim 10^6\ K$ at the stellar surface), $\rho_o = 10^{13}$ particles$/cm^3$, $A = 10^3$, $\mu = 1$ which correspond to $\omega \sim 6.2$, $\nu \sim 26.3$ while the ratio of Eq.(29) is $\Lambda = 1.8$.

We use a "minimal" radiative law so that F_{rad} is equal to gravity at the stellar surface but drops as R^{-3} with distance (i.e. much faster than gravity) (Fig. 3b). The employment of such radial dependence for the radiative force in optically thin atmospheres is possible after the discussion of Chen & Marlborough 1994 (see comments in next section). The motivation of this example is to show that even a *"minimal"* incorporation of radiation force produce a significant influence to the thermally driven solution. In Fig. 3 the radial velocity profiles (Fig. 3a) and the force balance (Fig. 3b) are shown. The centrifugal force contribution is two or three orders of magnitude smaller than the thermal and radiative forces so the wind is thermally driven in this application. The outward force, shown in the same figure, is the total sum of the outward forces (thermal plus radiative plus centrifugal) and its intersection with the gravity line separates the stellar surrounding into the flow acceleration and deceleration region respectively. The radial velocity change is significant even for this *minimal radiative law* (Fig. 3a). The wind initiates with the same initial radial velocity ($\sim$ 50 km/sec) but after the acceleration region reaches a maximum radial velocity ($\sim$ 120 km/sec) larger than KM case and the following deceleration is much slower.

In Appendix B, the role of the centrifugal force in the present solution driving is discussed and it is found to be negligible for the majority of the stars. A main assumption for this discussion is that the stars have not accretion disks and the fluid rotational velocity is equal to the star's rotation at the stellar surface. The helicoidal flow hypothesis permits only the inverse distance dependence for the azimuthal velocity ($V_\phi \propto 1/R$) which expresses the angular momentum conservation. This dependence originally differs from the Keplerian rotation used in other works. The dimensionless ratio Λ is a measure of the rotation versus thermal parameter

$$\Lambda = \frac{c^2\omega^2}{c\nu^2/2} = c\frac{R_o V_{rot}^2}{GM} = \Lambda_o \frac{R_o}{M}\frac{V_{rot}^3}{\sqrt{T_p}} \quad \text{for } Range\ I \qquad (29)$$

and it is evaluated for many types of stars. The result is shown in Table 2 and Fig. 6 of Appendix B.

The analysis presented in this section, is that a *fully analytical 2-D model* for *thermally plus radiatively* driven winds is obtained for *any* R-dependence of the radiative force acting in optically thin stellar atmospheres. In the next section, this 2-D model is applied to massive winds of B supergiants under several considerations of the R-profile of the radiative force deducing the wind transition from a strong radiation driving to a pure non radiative, thermally driven case.

3. Applications to outflows from B stars

In this section we use the *solution* in *Range I* for radiatively and thermally driven winds in order to describe the stellar winds of B type supergiants (B5I). It is evident that the late type main-sequence stars (the Sun is an illustrative example) are very slow rotators due to the *magnetic braking* and the wind is practically transparent to the stellar radiation due to the low density, so, our 2-D HD model fails to describe them. However, in B supergiants the absorption of the stellar radiation by the fluid is important and the radiative force given by (25) approximates the influence of the stellar radiation on the outflow supposing that the atmosphere is optically thin. The optically thin atmosphere approximation is much more appropriate to stars with high mass-loss rate and low terminal velocity similar to P Cygni (Lamers 1986). In this cases the optically thick line driven models fail because they produce a self initiating excitation mechanism for the wind with a very sharp velocity profile (due to the Sobolev

Table 1. Parameters for the application of Fig. 4

case	A	$u_R^{in}(1,\pi/2)$ (km/sec)	Radiation law $Q(R)$
1	100	36	$F_{rad} \propto 1/R$
2	100	36	$F_{rad} \propto 1/R^2$
3	1200	125	$F_{rad} \propto 1/R^3$
4	100	36	$F_{rad} \propto e^{-R}$
5	900	108	$F_{rad} \propto e^{-R}/R$
6	900	108	$F_{rad} \propto e^{1/R}/R^2$

approximation) connecting the high mass loss rate with high ($> 10^3\ km/sec$) outflow velocities.

Moreover, B supergiants have low escape velocities (low ν in the solutions), typical coronal temperatures of $10^5\ K$ - $10^6\ K$ near the stellar surface, particle densities $\sim 10^{10}-10^{11}\ p.cm^{-3}$, and maximum outflow velocities $\sim 400\ km/sec$ (for example 440 km/sec for 67 Oph, 410 km/sec for η CMa etc.). The observed mass loss rates for B supergiants range from a few $10^{-7}\ M_\odot/yr$ to a few $10^{-6}\ M_\odot/yr$ (Underhill & Doazan 1982, p 101, 146, 246).

In Fig. 4 an application is shown for a B5I supergiant of

$$M = 20\ M_\odot,\ R = 50\ R_\odot,\ V_{rot} = 35\ km/sec$$

using the parameters: $T_p = 5\ 10^3\ K$ (gives surface temperature of the order of $\sim 10^5 - 10^6\ K$), $\rho_o = 10^{11}\ part/cm^{-3}$, $\mu = 1$ which correspond to $\omega = 3.87$, $\nu = 43$, $\Lambda = 1.7$ and the values of Table 1.

The *"radiation laws"* used for this application, shown in Table 1, are determinations of the function $Q(R)$ (Eq. 25). The constant F_o in the same equation, has been chosen in order to be equal the radiative acceleration and gravitational deceleration at the stellar surface (Fig. 4b). In this case and assuming that the mechanism of the light absorption is the pure Thomson scattering by the free plasma electrons, the central object possesses the Eddington luminosity (Eq. 26). All functions $Q(R)$, chosen for application, decay monotonically with distance but in different ways.

As already mentioned in paragraph 2.2, the radiative force can be analyzed in the continuum and linear parts (Eq. 22). The part due to the continuum spectrum is proportional to R^{-2}. According to Chen & Marlborough 1994, after an optically thin hypothesis, the $f_{rad}^{ThinLines}$ part of the force can be expressed as $W(R)/R^2$ where W is a function of distance depending upon the local excitation and ionization equilibrium. Lamers 1986 first discussed this case in order to explain the Be stars winds, concluding that the radiative acceleration in an optically thin atmosphere could be represented by an inverse squared law with $W = const.$ However, Chen & Marlborough 1994 pointed out that $W = const.$ gives a too dense equatorial plane for Be stars and proposed that W should increase with distance adopting a power law dependence of the form:

$$a_{rad} \propto \frac{1}{R^2}\ \eta\ R^\epsilon \propto \frac{C}{R^{2-\epsilon}} \tag{30}$$

with η, ϵ, C constants. The authors discussed the values of the constants based on the location of the sonic point (i.e. in order that the wind originates subsonic close to the star and terminates supersonic). The authors suggest values of ϵ less than unity.

The considered radiation forces for this application are in accordance with previous works. First, in case 2 we apply the classic case of R^{-2} radiative dependence, appearing in pure Thomson scattering, where the radiative force balances gravity at every distance. Furthermore, let us consider cases 1 and 3 using R^{-1} and R^{-3} dependences in radiative law which correspond to $\epsilon = \pm 1$ in Eq. (30) and illustrate a high radiative and an approximately non-radiative situation. Through cases 1-3 the behaviour of the wind upon the relative strength of radiative force is deduced. Moreover, let us consider the pure exponential dependence (case 4) and exponential deviations from power laws (cases 5, 6) (all these laws are shown in Fig. 4b). The chosen examples fulfill (except case 1) our purpose which is not to create a strong radiative model (although it is possible by appropriate F_o and $Q(R)$, paragraph 2.2) but to keep a significant thermal driving in the wind. Case 4 is of special interest because it is transitional between cases 1 and 3 illustrating a radiative acceleration which dominates gravity from the star's surface up to a certain distance but after this it drops very faster than gravity, so the radiative effect could be neglected after a certain distance from the star. For strict applications to real objects $Q(R)$ has to be defined possibly by spectroscopic observational data.

The mass loss rate $\dot{M}$ is:

$$\dot{M} = \int\int_S \rho \mathbf{u}_R d\mathbf{s} \tag{31}$$

with S a closed surface containing the star. It is found that $\dot{M} = 4\pi R_o^2 \rho_o V_p \simeq 3.7\ 10^{-7}\ M_\odot/yr$ for this application, which is very close to observed mass loss rate $\dot{M}$ for B supergiants. We have to note that this is a *minimum estimation* of the mass loss rate because we assumed that the wind consists of pure hydrogen. The presence of heavier ions increases the mass loss rate. In order to obtain larger $\dot{M}$, we can also use a greater value of T_p which increases V_p (but giving no greater than $10^6\ K$ coronal temperature near the star), and greater value for ρ_o without overtaking the observed value ($\sim$ a few times $10^{11}\ part.cm^{-3}$) at the coronal base.

The application of *Range I* solution (Sect. 2.1) to B5I supergiant is illustrated in Fig. 4. In (a) the radial velocity profiles for the cases of Table 1 are shown. The chosen parameters A produce the lowest initial values of V_R (i.e $u_R^{in}(1,\pi/2)$) in each case. The respective dimensionless radiative accelerations in comparison with the gravitational deceleration (dashed line) is shown in plot (b). It is clear that in cases 1, 2, 4 where the radiative force dominates or counters gravity the initial velocity is lower ($\sim$ 35 km/sec). In cases 1 and 2 where the radiative force dominates or balances gravity everywhere the wind is accelerated continuously up to infinity. In the other cases, a deceleration region always exist after a certain distance where gravity dominates the total outward force (thermal plus radiative plus centrifugal). For a given initial velocity, the highest outflow velocity is obtained in cases 1 and 4 where exists a region of

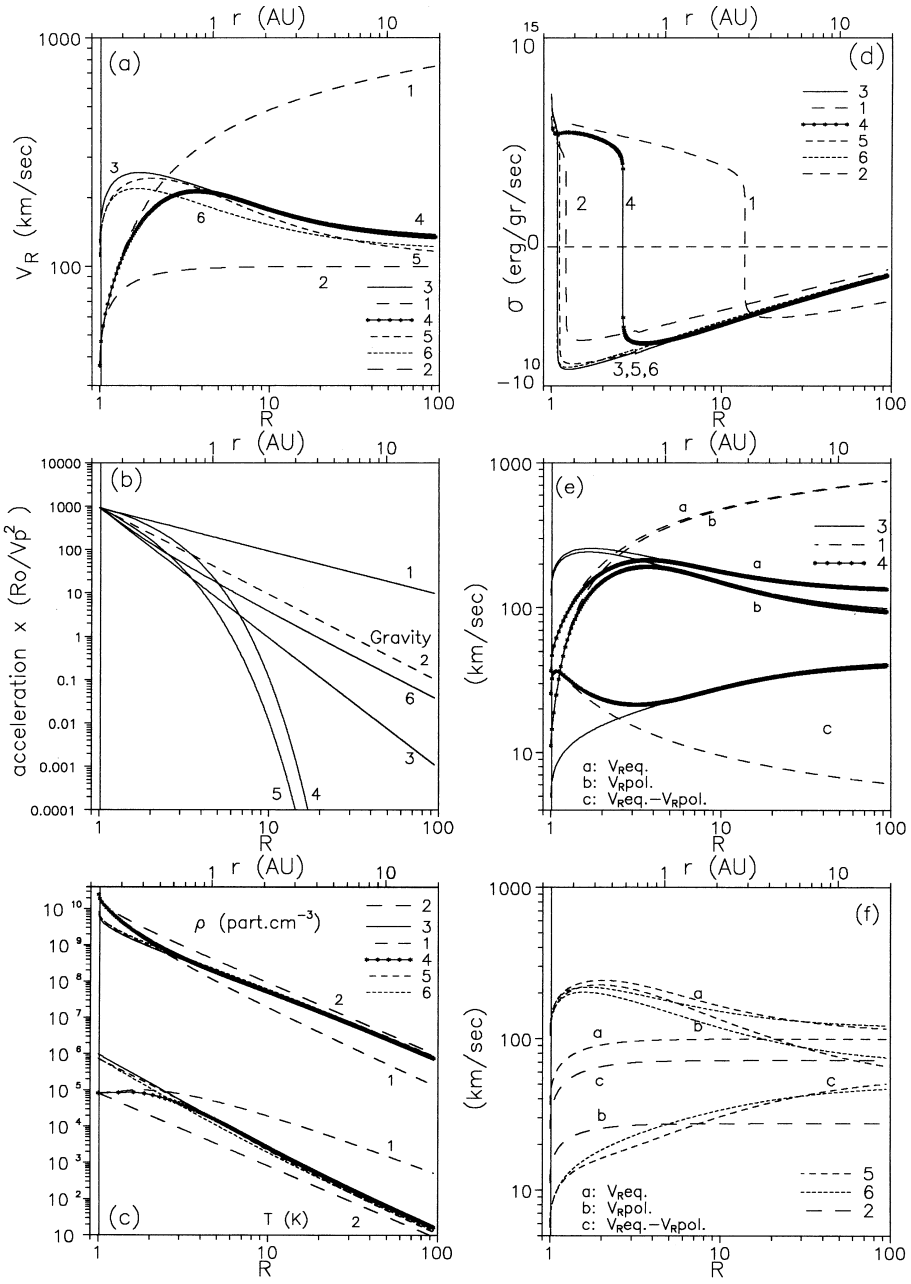

Fig. 4a–f. Application of the solution in *Range I* for a thermally and radiatively driven wind from a B5I supergiant considering several R-dependences of the radiative force (Eq. 25, Table 1). **a** radial velocity profiles **b** dimensionless radiative acceleration (in V_p^2/R_o units). The dashed line shows the R^{-2} dependence of the gravitational deceleration **c** density ρ and temperature T profiles **d** heating function σ profiles **e**, **f** dependence of the radial velocity asymmetry (curves c) between equator $V_{R/eq}$ (curves (a)) and poles $V_{R/pol}$ (curves (b)) (curves (c) represent the difference $V_{R/eq} - V_{R/pol}$) **e** cases 1,3,4 **f** cases 2,5,6

radiative domination towards gravity close to the central object (maximum V_R is $\sim$ 800 km/sec at 100 R_o in case 1). In case 3 the radiative effect is negligible giving a maximum outflow velocity of $\sim$ 250 km/sec and the velocity profile tends to the non-radiative case. In case 4 the velocity profile tends to case 1 close to the star but deviates from it after 0.5 R_o and finally follows the case 3 profile after 7 R_o. This happens because of the used exponential radiative law which produces high and dominating radiative acceleration towards gravity close to the star and negligible at larger distances.

In Fig. 4 (e),(f) the radial velocity difference (curves c) between the stellar equator $V_{R/eq}$ (curves a) and poles $V_{R/pol}$ (curves b) is plotted as a function of radial distance R. It is seen from curves c which represent the difference $V_{R/eq} - V_{R/pol}$, that in case 1 there is an initial asymmetry between equatorial and polar values which vanishes with distance while in case 3 the asymmetry close to the star is negligible and increases with R. In case 2 the asymmetry increases close to the star and remains approximately constant after a certain distance. Consequently, the domination of the radiative force leads to radial flow and this result is due to the radiality of the radiative acceleration. In the transitional case 4 the asymmetry is large in both close and far regions with a minimum at $\sim$ 2 R_o. In cases 4 and 5 the asymmetry behaves similar to case 3.

In Fig. 4c the temperature and density profiles are shown. The density close to the star is about 10^{10} $part/cm^3$ and 10^8 $part/cm^3$ at 10 stellar radii which is consistent with observations (Underhill & Doazan 1982, p.246), dropping to

$10^5\ part./cm^3$ at 100 $R_\odot$. The temperature at the coronal base is $\simeq 10^5\ K$ when the radiative force is important (cases 1,2,4) and $\simeq 10^6\ K$ when the radiative force is small (cases 3,5,6). These values coincide with observations too (Underhill & Doazan 1982, p.246). It is also seen that the temperature drops slower in radiative cases (note that the temperature is approximately constant close to the star in cases 1 and 4) and this result is expected because of the radiative heating due to the light absorption by the fluid. The heating function σ (Fig. 4d) supports the last remark giving larger heating regions in cases where the radiative acceleration dominates (i.e. the heating region in case 1 is broadened compared with case 3 and heating regions of cases 1 and 4 are extensive compared with cases 3,5,6). In all cases, fluid cooling follows the heating regions.

A basic problem in stellar winds is to find out the total physical mechanisms which produce the necessary heating for the flow. This problem is also important for the solar wind (lots of *in situ* measurements by the space probes are available for this flow!) concerning both polytropic or non-polytropic models. In our case and in order to explain a part of the estimated heating σ, we could adopt similar to the solar wind mechanisms as heating by waves (magnetoacoustic, Alfvénic or other MHD waves), magnetic twisting and relaxation at the stellar surface, absorption of the stellar light etc. Some of the fluid cooling could also be radiative cooling since the fluid radiates as a black body of temperature $T(R,\theta)$. If the cooling is radiative and in the presence of metals combined with high plasma density, some emission lines could form at the stellar spectrum connecting the heating function obtained here with the P Cygni (emission/absorption) profiles usually observed in B stars. About the importance of the acoustic waves absorption in stellar winds we must note that they are usually employed not only in the energy budget but as a momentum addition source as well. Koninx & Hearn 1992 presented a 1-D numerical model for Be star winds driven by both radiation and acoustic waves dissipation which are very important in the equatorial plane of Be stars. The inclusion of the acoustic waves force combined with the Sobolev approximation increases the mass loss rates and decreases the outflow velocities because it creates lower velocity gradients. The acoustic waves in this model may explain a part of the needed energy but we consider that they do not contribute to the equation of motion. Finally, we have to note that the way that σ is introduced in the energetics carries no *a priori* assumptions but this function is evaluated self-consistently *a posteriori* from the solutions representing the external energy that is necessary for the flow existence. As seen from Fig. 4d, σ is remarkably sensitive upon radiative force changes. This behaviour suggests a connection of this function with the radiation absorption mechanisms. The temperature is also sensitive upon the radiation law (Fig. 4c) It is remarkable that while no *a priori* isothermal condition is used, in strong radiative cases the temperature profile exhibits a plateau close to the star indicating that isothermality and LTE (often used in strong radiative numerical models) are good approximations. These self-consistent results are in excellent agreement with our expectations for a thermally plus radiatively driven 2-D model.

In all above cases the wind becomes supersonic very close to the star through a spherical sonic surface (Sect. 2.1). As a conclusion for the application, we note that the radiative force is very important in excitation and driving of massive winds from B supergiants, implying low initial radial velocity and accelerating efficiently the wind to high outflow velocities giving asymptotically radial V_R.

4. Summary and discussion

The work of this article concerns the 2-D HD outflows from central astrophysical objects presenting global, self-consistent, *fully analytical solutions* to cases in which both thermal pressure gradient and radiative force (in optically thin atmosphere) are significant in the wind excitation and driving. The basic characteristics of this 2-D model, which extends the pure thermally driven solution of KM, are:

- axisymmetry and helicoidal streamline geometry with radial asymptotes
- evaluation of the complete force balance at every distance (i.e. gravity, thermal pressure gradient, centrifugal and radiative)
- generalized differential rotation for the fluid
- initially subsonic outflow which becomes supersonic close to the star
- incorporation of the radiative force under the assumption of optically thin atmosphere
- simplicity in the mass loss rate $\dot{M}$ derivation

We note that the centrifugal force contribution is found negligible since magnetic field and accretion disks are absent and the wind's angular momentum is offered by the rotating central object and it is conserved in the fluid (see Appendix B). The centrifugal force generally helps a thermally driven wind to start from the stellar surface which is generally problematic in massive winds of slowly rotating or non rotating stars. We must note that in order to explain the mass-loss from early type stars empirically, a "critical rotational velocity" (also named as *break-up* velocity) ($V^*_{rot} = \sqrt{GM/R}$) has been introduced to equal the centrifugal force and the gravity at the stellar surface. However, this "critical rotational velocity" is not observed in early type stars (Underhill & Doazan 1982, p. 294, 362) so the necessity of such a critical velocity is just indicative for the wind excitation problem. On the other hand, centrifugally or magnetically driven models have been developed to describe the excitation of winds and jets from accretion disks (Blandford & Payne 1982, Contopoulos & Lovelace 1994, Contopoulos 1995) and these models apply to YSOs and AGNs where bipolar collimated jets and accretion disks seem to coexist. In these models the role of the centrifugal force in the wind driving is different and the presence of the azimuthal magnetic field is crucial for the acceleration.

In the present model the decrease of the initial velocity compared with Paper I is possible with the inclusion of the radiative force. When the radiative force is significant compared with gravity, much smaller initial velocity is necessary for the wind

excitation. In the case of radiatively driven wind, the initial velocity is minimum. We have to note here that pure HD models exhibit generally difficulty in reproducing the initial acceleration at the stellar surface (needed for the flow) and the stellar magnetic field (full MHD) plays possibly an important role there.

The present model seems to exhibit some advantages compared with respective radiative models. The 1-D and 2-D line driven radiative models are numerical, often using the Sobolev approximation. In the original work of Castor et al. 1975 (CAK) they presented 1-D numerical results of radiatively driven stellar winds and applied their model to an O5f main-sequence star of 60 $M_\odot$ and 14 $R_\odot$ obtaining terminal velocities of $\sim$ 1.5 10^3 km/sec and mass-loss rate of 6 10^{-6} $M_\odot/yr$. In their work, they used a radiation force (depend on the optically thick lines) acting in a spherically distributed stellar corona ignoring the rotation of the star. A very sharp velocity versus radial distance profile starting from zero at the stellar surface and reaching 10^3 km/sec after negligible radial distance was obtained. Improvements have been made in CAK model in order to apply in Be stars which show a dense equatorial disk expanding with low velocity ($\sim$ 200 km/sec). The incorporation of the rotation in CAK model produces smoother profiles and lower terminal velocities (Poe & Friend 1986). As already mentioned, Koninx & Hearn 1992 suggested an alternative radiation plus acoustic waves driving mechanism. Chen et al. 1992 model the Be stars using power law profile for the radiative force and empirical β or power law profiles for the velocity. Bjorkman & Cassinelli 1993 presented a 2-D model in which the wind concentrates to the equatorial plane in order to describe Be stars. This 2-D work provides analytic information about the physical mechanism of the equatorial concentration in Be stars and Owocki et al. 1994 developed a powerful 2-D numerical solution based in Bjorkman & Cassinelli model for Be stars validating in general their results. Accurate 2-D numerical solutions for Be stars were given by Arauzo & Freitas Pacheco 1989. Arauzo 1995 solved numerically the equations in the equatorial plane approximating the case of thin lines driving (α = 0). All previous works improve the CAK model and give in different ways consistent results with observations of Be stars. However, their numerical nature hides many technical difficulties in implementation (e.g. Owocki et al. 1994). Additionally, a usual assumption in these models is the wind isothermality and LTE although in CAK model the temperature scales with distance. Our model originally differs by offering an alternative *thermal plus radiation mechanism* in driving the wind without any assumption on the temperature. The analytical self-consistent solutions indicate that the temperature gradient varies with the adopted radiation mechanism. Besides, empirical β or power laws for the velocity are avoided.

In Sect. 3 our *thermally and radiatively driven fully analytical 2-D solution* applied to B5I supergiants assuming an optically thin stellar atmosphere and considering the basic electron opacity law and deviations from it. As seen in Fig. 4, maximum outflow velocities ranging from 250 to 800 km/sec obtained depending upon the radiative acceleration profile while a *minimum* mas loss rate of 3.7 10^{-7} $M_\odot/yr$ is estimated. The radial velocity asymmetry between the equator and the poles increases with R when the radiative acceleration is negligible and diminishes with R when the radiative force dominates. It seems that the radiative mechanism is very important in winds from evolved massive stars and an accurate "radiative law" based on observations is necessary.

Acknowledgements. A.Kakouris acknowledges the Greek State Scholarships Foundation (**SSF:IKY**) for his scholarship. Both authors are grateful to J.Polygiannakis and A.Alevizos for stimulating discussions and to Dr. C.Sauty who improved the final version of this article with his useful comments.

Appendix A: geometrical generalization in Paper I solution

Searching for self-consistent solutions of Eqs (1) - (4), we could generalize the solution given by Kakouris & Moussas 1996 (Paper I) supposing the velocity θ-dependence given by Eqs (5, which include a new parameter μ giving the Paper I case for μ = 1. Substituting these expressions in (Eq. 2) and using Eq. (8) we obtain:

$$\left[\left(g(R)+\frac{\omega^2}{R^2}\right)\left(-\frac{\nu^2}{2R^2}-\frac{1}{2}\frac{df}{dR}\right)+\frac{dg}{dR}f(R)\right]\cdot$$

$$\mu\ \sin^{2\mu-1}\theta\ \cos\theta+$$

$$\left[-\frac{1}{2}\frac{dg}{dR}\left(g(R)+\frac{\omega^2}{R^2}\right)\right]\ \mu\ \sin^{4\mu-1}\theta\ \cos\theta\ =$$

$$\left[-4\frac{\omega^2}{R^3}f(R)-\frac{1}{2}\frac{\omega^2}{R^2}\frac{df}{dR}\right]\ \sin^{2\mu-1}\theta\ \cos\theta+$$

$$\left[\frac{\omega^2}{R^3}\left(g(R)+\frac{\omega^2}{R^2}\right)+\frac{1}{2}\frac{\omega^2}{R^2}\left(\frac{dg}{dR}-2\frac{\omega^2}{R^3}\right)\right]\cdot$$

$$\sin^{4\mu-1}\theta\ \cos\theta \tag{A1}$$

Setting the coefficients of $\sin^{4\mu-1}\theta\cos\theta$ and $\sin^{2\mu-1}\theta\cos\theta$ equal to zero we obtain, respectively, a set of two ODE for $f(R)$ and $g(R)$. One of them (coming from the coefficients of $\sin^{4\mu-1}\theta\ \cos\theta$) contains $g(R)$ solely and integrated gives (Eq. 10):

$$g(R)=\frac{\xi-(\mu+1)\omega^2}{\mu R^2}$$

where the new variable ξ is related to the radial distance R as (Eq. 14):

$$(cR)^{2(\mu+3)}=\frac{|\xi-(\mu+4)\omega^2|^{(\mu+4)}}{|\xi-\omega^2|}$$

with c a positive constant. We note that this is the general case, giving the Paper I transformation for μ = 1. In Fig. 5 this generalized behaviour of $\xi(R)$ is shown, allowing again to split into four individual intervals of ξ where R is unbounded, single

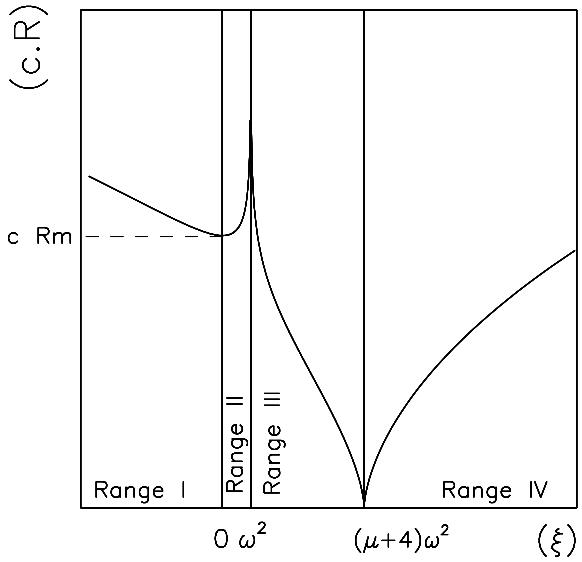

Fig. 5. Types of solutions. Demanding R to be single valued and unbounded (i.e. infinitely large) we can use one of the (Range I - Range IV) four intervals of ξ obtaining four types of independent solutions. When μ equals to unity, this diagram gives the respective Paper I case.

valued and the solutions independent. We call every interval as *Range* of solutions, similar to Paper I, so:

Range I : $(-\infty, 0)$, Range II : $(0, \omega^2)$,

Range III : $(\omega^2, (\mu+4)\omega^2)$, Range IV : $((\mu+4)\omega^2, +\infty)$

Substituting the previous functions in the other ODE which contains $f(R)$ (coming from the vanishing of the $\sin^{2\mu-1}\theta\ \cos\theta$ coefficients) we get (Eq. 9):

$$f(R) = f_{\rm o}(\xi)[A + A_1 I_1(\xi)]$$

with (Eq. 11)

$$f_{\rm o} = \frac{|\xi-\omega^2|^{\frac{2(\mu+2)}{\mu+3}}}{|\xi-2\omega^2|^{\frac{2\mu}{\mu+2}}|\xi-(\mu+4)\omega^2|^{\frac{2(\mu+4)}{(\mu+3)(\mu+2)}}}$$

where A is an integration constant, $A_1 = c\nu^2/2$ and $I(\xi) = \int Y_1(\xi)d\xi$ (evaluated by Simpson's rule) with (Eq. 13):

$$Y_1(\xi) = \frac{-\xi}{(\xi-(\mu+4)\omega^2)(\xi-2\omega^2)}\cdot$$

$$\frac{|\xi-(\mu+4)\omega^2|^{-\frac{(\mu-2)(\mu+4)}{2(\mu+3)(\mu+2)}}|\xi-2\omega^2|^{\frac{2\mu}{\mu+2}}}{|\xi-\omega^2|^{\frac{4\mu+7}{2(\mu+3)}}}$$

Integrating Eq. (2), the flow pressure $P(R,\theta)$ is derived introducing the constant $P_o = 2k_B T_p \rho_o/m_p$:

$$P(R,\theta) = P_o[\mathscr{A} - \frac{\omega^2}{R^2(\xi-\omega^2)}\sqrt{f - \frac{\xi-\omega^2}{\mu R^2}\ \sin^{2\mu}\theta}] \quad \text{(A2)}$$

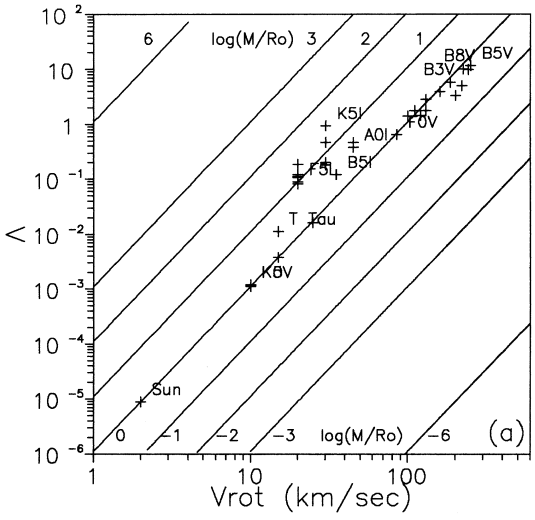

Fig. 6. Dependence of the ratio Λ (Eq. 29) upon the stellar mass M, radius $R_{\rm o}$, rotational velocity V_{rot} and atmospheric temperature ($T_p = 10^4\ K$ which gives $\sim 10^6\ K$ surface temperatures). Every solid line corresponds to a constant value of $M/R_{\rm o}$.

where $\mathscr{A}$ is an integration constant, while from the equation of state (Eq. 4) the temperature is found to be:

$$T(R,\theta) = T_p[\mathscr{A}R^2\sqrt{f(R) - \frac{\xi-\omega^2}{\mu R^2}\ \sin^{2\mu}\theta} -$$

$$-\frac{\omega^2 f(R)}{\xi-\omega^2} + \frac{\omega^2}{\mu R^2}\ \sin^{2\mu}\theta] \quad \text{(A3)}$$

The radial Mach number (i.e. ratio of the radial flow velocity to the local speed of sound V_s), is ($\gamma = 5/3$):

$$\mathscr{M}(R,\theta) = \frac{u_R}{V_s} = \frac{u_R}{\sqrt{\gamma\ P/\rho}} =$$

$$\left[\frac{f - \frac{\xi-\omega^2}{\mu R^2}\ \sin^{2\mu}\theta}{\frac{5}{3}[\mathscr{A}R^2\sqrt{f - \frac{\xi-\omega^2}{\mu R^2}\ \sin^{2\mu}\theta} - \frac{\omega^2 f}{\xi-\omega^2} + \frac{\omega^2}{\mu R^2}\ \sin^{2\mu}\theta]}\right]^{\frac{1}{2}} \quad \text{(A4)}$$

Once the basic flow quantities were found analytically we can derive any other flow quantity as well.

Appendix B: estimation of the ratio Λ for several types of stars

The effect of the centrifugal action in the outflow is studied through the deduction of the ratio Λ (Eq. 29) for several types of stars

$$\Lambda = \Lambda_o \frac{R_{\rm o}}{M}\frac{V_{rot}^3}{\sqrt{T_p}}$$

For the next table, (data from Lang 1992, Bertout 1989 were used and temperature parameter $T_p = 10^4$ which gives $\sim 10^6\ K$ temperature at the stellar surface). In Fig. 6 the ratio Λ versus

Table 2. Dependence of ratio Λ upon stellar parameters

Type	M $(M_\odot)$	R_o $(R_\odot)$	V_{rot} (km/s)	Λ	ω
O8V	23	8.5	200	3.3	15.6
O8I	28	20	130	1.7	10.1
B0V	17.5	7.4	220	5.0	17.2
B0III	20	15	120	1.4	9.4
B0I	25	30	110	1.8	8.6
B3V	7.6	4.8	240	9.7	18.7
B5V	5.9	3.9	250	11.5	19.5
B5III	7	8	130	2.8	10.1
B5I	20	50	35	0.2	2.7
B8V	3.8	3	225	10.0	17.6
A0V	2.9	2.4	185	5.8	14.4
A0III	4	5	100	1.4	7.8
A0I	16	60	45	0.4	3.5
A5V	2	1.7	160	3.9	12.5
A5I	13	60	45	0.5	3.5
F0V	1.6	1.5	85	0.6	6.6
F0I	12	80	30	0.2	2.3
F5V	1.4	1.3	25	$1.6\ 10^{-2}$	1.9
F5I	10	100	20	$9\ 10^{-2}$	1.5
G0V	1.05	1.1	10	$0.1\ 10^{-2}$	0.8
G0III	1	6	30	0.2	2.3
G0I	10	120	20	0.1	1.5
G5V	0.92	0.92	10	$0.1\ 10^{-2}$	0.8
Sun	1	1	2	$9\ 10^{-6}$	0.1
G5III	1.1	10	20	$8\ 10^{-2}$	1.5
G5I	12	150	20	0.1	1.5
K0V	0.79	0.85	10	$0.1\ 10^{-2}$	0.8
K0III	1.1	15	20	0.1	1.5
K0I	13	200	30	0.5	2.3
K5V	0.67	0.72	10	$0.1\ 10^{-2}$	0.8
K5III	1.2	25	20	0.2	1.5
K5I	13	400	30	0.9	2.3
T Tau	1	1	15	$0.4\ 10^{-2}$	1.2
T Tau	1	3	15	$1.1\ 10^{-2}$	1.2

rotation is shown and some types of stars are also indicated. It is seen that the maximum Λ value (~ 12) is estimated for B5V stars which are very fast rotators, a value of (~ 10) is obtained for B3V and B8V stars, and the minimum ($\sim 10^{-5}$) for the Sun. Consequently, the centrifugal influence in the solutions presented in this work is negligible.

References

Abbott, D.C., 1982, ApJ, **259**, 282 – 301

de Araujo, F.X., 1995, A&A, **298**, 179 – 186

de Araujo, F.X., de Freitas Pacheco, J.A., 1989, MNRAS, **241**, 543 – 557

Bertout, C., 1989, ARA&A, **27**, 351 – 395

Bjorkman, J.E., Cassinelli, J.P., 1993, ApJ, **409**, 429 – 449

Blandford, R.D, Payne, D.G, 1982, MNRAS, **199**, 883 - 903

Bondi, H., 1952, MNRAS, **112**, 195 – 204

Bryce, M., Balick, B., Meaburn, J., 1994, MNRAS, **266**, 721 – 732

Cassinelli, J.P., 1979, ARA&A, **17**, 275 – 308

Castor, J.I, Abbott, D.C, Klein, R.I, 1975, ApJ, **195**, 157 – 174

Chen, H., Marlborough, J.M., Waters, L.B.F.M., 1992, ApJ, **384**, 605 – 612

Chen, H., Marlborough, J.M., 1994, ApJ, **427**, 1005 – 1012

Contopoulos, J., 1995, ApJ, **450**, 616 – 627

Contopoulos, J., Lovelace, R.V.E., 1994, ApJ, **429**, 139 - 152

Friend, D.B., Abott, D.C., 1986, ApJ, **311**, 701

Gonzalez, J.F., LeBlanc, F., Artru, M.C., Michaud, G., 1995, A&A, **297**, 223 – 236

Hughes, P.A, (editor), 1991, " *Beams and Jets in Astrophysics*", Cambridge Astrophysics Series, 484 – 564

Kakouris, A., Moussas, X., 1996, A&A, **306**, 537 – 546

Koninx, J.P.M., Hearn, A.G., 1992, A&A, **263**, 208 – 218

de Kool, M., Begelman, M.C., 1996, ApJ, in press

Kudritzki, R.P., 1992, A&A, **266**, 395 – 401

Kudritzki, R.P., Pauldrach, A., Puls, J., Abbott, D.C., 1989, A&A, **219**, 205 – 218

Lamers, H.J.G.L.M, 1986, A&A, **159**, 90 – 100

Lang, K.R., 1992, "*Astrophysical Data: Planets and Stars*", Springer Verlag, p. 132 – 147

Lima, J.J.G., Priest, E.R., 1993, A&A, **268**, 641 – 649

Lima, J.J.G., Tsinganos, K., 1996, Geoph.Res.Lett., **23**, No.2, 117 –120

Owocki, S.P., Cranmer, S.R., Blondin, J.M., 1994, ApJ, **424**, 887 – 904

Parker, E.N., 1958, ApJ, **128**, 664 – 676

Phillips, J.L., Bame, S.J., Feldman, W.C., Goldstein, B.E., Gosling, J.T., Hammond, C.M., McComas, D.J., Neugebauer, M., Scime, E.E., Suess S.T., 1995, Science, **268**, 1030 – 1033

Poe, C.H., Friend, D.B., 1986, ApJ, **311**, 317 – 325

Sauty, C., 1994, Ann.Phys.Fr., **19**, 459 – 599

Tsinganos, K., Vlastou-Tsinganos, G., 1988, A&A, **193**, 125 – 130

Tsinganos, K., Trussoni, E., 1990, A&A, **231**, 270 – 276

Tsinganos, K., Sauty, C., 1992, A&A, **255**, 405 – 419

Underhill, A., Doazan, V., 1982, "*B stars with and without emission lines*", Monograph Series on Nonthermal phenomena in Stellar Atmospheres, NASA

This article was processed by the author using Springer-Verlag LaTeX A&A style file *L-AA* version 3.